Four-photon orbital angular momentum entanglement

B. C. Hiesmayr,[1] M. J. A. de Dood,[2] and W. Löffler[2, *]

[1] *University of Vienna, Faculty of Physics, Boltzmanngasse 5, A-1090 Vienna, Austria*

[2] *Huygens–Kamerlingh Onnes Laboratory, Leiden University,*
P.O. Box 9504, 2300 RA Leiden, The Netherlands

Quantum entanglement shared between more than two particles is essential to foundational questions in quantum mechanics, and upcoming quantum information technologies. So far, up to 14 two-dimensional qubits have been entangled,[1,2] and an open question remains if one can also demonstrate entanglement of higher-dimensional discrete properties of more than two particles.[3,4] A promising route is the use of the photon orbital angular momentum (OAM), which enables implementation of novel quantum information protocols,[5,6] and the study of fundamentally new quantum states.[7,8] To date, only two of such multidimensional particles have been entangled[9] albeit with ever increasing dimensionality.[10–12] Here we use pulsed spontaneous parametric downconversion (SPDC)[13] to produce photon quadruplets that are entangled in their OAM, or transverse-mode degrees of freedom; and witness genuine multipartite Dicke-type entanglement.[14,15] Apart from addressing foundational questions,[16] this could find applications in quantum metrology, imaging, and secret sharing.[17,18]

Twin photons that are created by SPDC are correlated in several degrees of freedom and exhibit quantum entanglement. Apart from the well-known polarization degrees, the photons can also be correlated in their spatial degrees; this manifests itself in continuous wavevector or (the Fourier-related) position entanglement.[19] We can also explore the spatial correlations using transverse paraxial optical modes, which can be chosen to form a discrete, orthogonal, and complete set, which is very useful for quantum information applications. In contrast to the 2-dimensional polarization space, the transverse mode space is in principle infinite dimensional, only limited by diffraction and the transverse size of optical components. Recently the use of computer-controlled holograms enabled steep increase of the single-particle Hilbert space up to 100 dimensions.[10,11] An experimentally useful choice of transverse modes are the Laguerre-Gauss (LG) modes where the azimuthal part factorizes and describes phase vortices $\exp(i\ell\phi)$, where ϕ is the azimuth and $\ell = -\infty \ldots \infty$ determines the twisting number of the wavefront; corresponding to an orbital angular momentum of $\ell\hbar$ per photon[20] (in addition to the spin angular momentum). The LG and the related Hermite-Gauss modes have well-known propagation dynamics, thus they are suitable for long-distance distribution of high-dimensional entanglement.

A photon pair produced by SPDC shows quantum entanglement in the transverse-mode and in particular the OAM degree of freedom,[9] this has already been used in a large number of quantum mechanical tests. The quantum correlations can be understood by considering the rotational symmetry of the SPDC process (on the wavelength scale, the crystal is rotationally symmetric); due to Noether's theorem, this leads to conservation of OAM. Therefore, we can write, in analogy to the well-known wavevector-space SPDC Hamiltonian, the OAM SPDC Hamiltonian in case of a Gaussian pump beam as

$$H = \sum_{\ell=-\infty}^{\infty} \frac{1}{2} i\kappa\hbar \left(a_\ell^\dagger a_{\bar{\ell}}^\dagger - a_\ell a_{\bar{\ell}} \right) \quad (1)$$

where $a_\ell^\dagger$ is the creation operator for a photon with OAM ℓ, $\bar{\ell} \equiv -\ell$ and κ describes the strength of the nonlinear interaction. A single SPDC photon pair is produced by the lowest-order term of the series expansion of $|\Psi\rangle = \exp(-it/\hbar H)|0\rangle$, leading to $|\Psi_2\rangle = \gamma \sum_{\ell=1}^{\infty} |1_\ell; 1_{\bar{\ell}}\rangle$ which describes two photons that are perfectly anticorrelated in their OAM[9,10] ($|n_k\rangle$ is a state with n photons in mode k). The single-pass amplitude gain $\gamma \propto \kappa t$ depends linearly on the pump beam intensity I_p. We explore here the next-order terms corresponding to the simultaneous production of 2 OAM photon pairs (for $\ell \neq 0$ modes):

$$|\Psi_4\rangle \propto \gamma^2 \left(\sum_{i,j=1,i\neq j}^{\infty} |1_{\ell_i}; 1_{\ell_j}; 1_{\bar{\ell}_i}; 1_{\bar{\ell}_j}\rangle + 2 \sum_{\ell=1}^{\infty} |2_\ell; 2_{\bar{\ell}}\rangle \right). \quad (2)$$

This state can be seen as a result of interference in a double-pair emission process, which for production of multiple photon pairs is much more stable than interferometric SPDC[13] experiments. Because the 4-photon term (Eq. 2) depends quadratically on the pump beam intensity, we use a picosecond pulsed laser, further we use 1 nm wide band pass filters for the downconverted photons to limit spectral (and temporal) labelling.[21] Since we use type-I SPDC, all produced photons have the same polarization. We use nonpolarizing beamsplitters to separate them, and a combination of phase-only spatial light modulation and projection onto the core of single mode fibers to perform projective measurements in transverse-mode space, see Fig. 1.

To study the SPDC produced state from Eq. 2, we record 4-photon correlations for different detection modes,
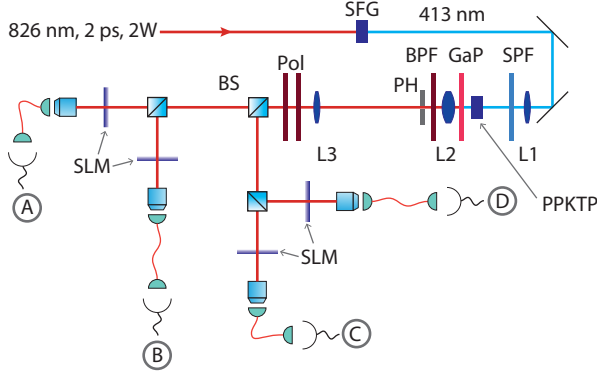
Figure 1. **Experimental implementation**. A frequency-doubled (SFG) mode-locked picosecond laser is short-pass filtered (SPF) and focussed (L1) into the periodically poled potassium titanyl phosphate (PPKTP) crystal. The SPDC photons are spectrally filtered with a GaP plate and a band-pass filter (BPF), and distributed with beam splitters (BS) to the 4 equal detection units. The crystal facet is imaged with a telescope (L2 & L3) onto the spatial light modulators (SLM), which in turn is far-field imaged onto the core of the detection single mode fibers connected to single photon counters. The pinhole (PH) selects the 1st diffraction order of the SLM holograms. We explore the 4-photon transverse-mode space by changing the holograms on the SLMs and recording 4-fold coincidence events with a multi-channel time tagging computer card.
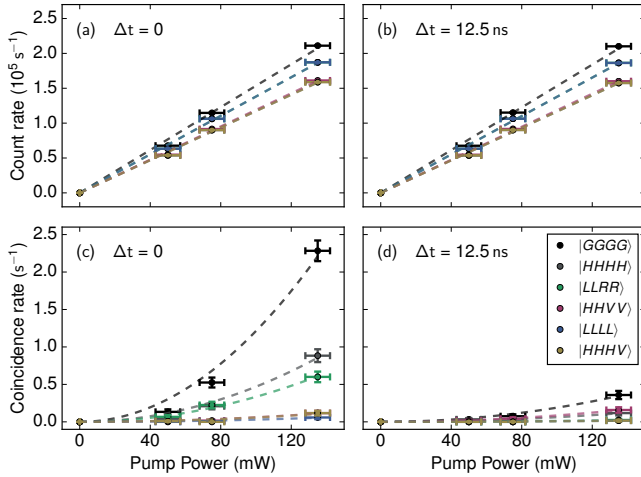

Figure 2. **4-photon OAM state production.** Pump-power dependent single-photon count rate (a, b) and 4-fold coincidence rate (c, d). The single rates depend linearly on pump power, while the 4-fold coincidences rates show quadratic dependency. The comparison between zero time delay (a, c) and the case where photon 3 and 4 are delayed by 12.5 ns shows that most detected 4-photon detection events are indeed due to 4 photons that were produced within a single pump pulse.
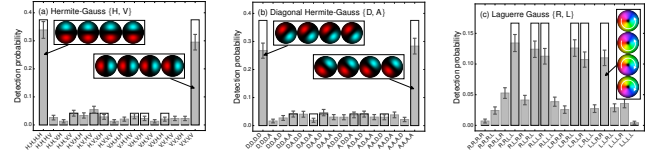

Figure 3. **4-photon OAM correlations.** 4-photon joint detection probabilities in each of the 3 mutually unbiased bases: Hermite-Gauss $\{H, V\}$, diagonal Hermite-Gauss $\{D, A\}$, and Laguerre Gauss $\{R, L\}$. Labels indicate the phase and amplitude structure of the detected spatial modes. Gray bars: experimental data, error bars show statistical errors. Boxes: theory. Experimental integration time per data point was 24 minutes. The probabilities are normalized to unity within each basis.

pump powers, and relative detection times, shown in Fig. 2. We restrict ourselves to the fundamental Gaussian (G) mode and the 2-dimensional first-order mode space. The 3 mutually unbiased bases of the latter are $\left\{LG_{+1}^0, LG_{-1}^1\right\} \equiv \{R, L\}$ in the Laguerre-Gauss basis, $\{HG_{0,1}, HG_{1,0}\} \equiv \{H, V\}$ in the Hermite-Gauss basis, and $\left\{HG_{0,1}^{45}, HG_{1,0}^{45}\right\} \equiv \{D, A\}$ in the 45° rotated Hermite-Gauss basis, in analogy to the polarization case.[22] We designed the experiment such that the single count rates depend only weakly on detection mode (Fig. 2 a, b). The 4-fold coincidence rate Γ for the case that all photons are produced by the same pump pulse (Fig. 2 c) is highest if all 4 photons are projected onto the fundamental Gaussian mode ($|GGGG\rangle$), and depends quadratically on the pump power as expected. From the ratio between (d) and (c), whereas in (d) detectors (A, B) and (C, D) are set to detect photons produced in two different laser pulses, we can estimate the fraction of uncorrelated events to be 10% ($\Gamma^{\Delta t=12.5ns}/\Gamma^{\Delta t=0}$). This is similar to the fraction of "forbidden" events (e.g., $\Gamma_{HHHV}/\Gamma_{HHHH} \approx 0.1$). We think the latter occur due to experimental imperfections; in contrast to polarization experiments we require here mode-matching between all 4 detectors and the pump beam simultaneously. This argument is supported by the fact that both ratios are largely independent on pump power, suggesting that contributions from higher-order multiphoton states are low.

These results support an intuitive explanation of the structure of Eq. 2, keeping in mind that the photons are produced in pairs: The first term in Eq. 2 that contains photons with different OAM $|\ell|$ occurs if the second pair is spontaneously emitted and uncorrelated to the first pair, while the second term corresponds to the case where the second pair is produced by a stimulated process giving a perfect clone of the first pair.[23–25] The different $|\ell|$ values in the first term in Eq. 2 is then simply a consequence of forbidden perfect quantum cloning, both terms together demonstrate the possibility of optimal quantum cloning in stimulated SPDC.[26]

Now we study the quantum correlations of the SPDC-produced 4-photon state, for which we focus on the 2-

dimensional first-order mode space with OAM $\ell = \pm 1$, and record 4-fold coincidences for all detector mode combinations in each basis. Fig. 3 compares experimental results and theoretical prediction for the SPDC-produced state, which becomes in this case (Eq. 2):

$$|\Psi_4^{(2)}\rangle \propto |2_\ell; 2_{\bar\ell}\rangle \qquad (3)$$

with $\ell = 1$. Note that Eq. 3 is valid for any ℓ, if we limit our detection to $\pm\ell$ modes, a 2D Hilbert space per photon. Experimentally, the beamsplitters generate all possible permutations of photons (Fig. 1), so $|\Psi_4^{(2)}\rangle$ becomes in the detector-basis

$$|D_4^{(2)}\rangle \propto |\ell\ell\bar\ell\bar\ell\rangle + |\ell\bar\ell\ell\bar\ell\rangle + |\bar\ell\ell\ell\bar\ell\rangle + |\ell\bar\ell\bar\ell\ell\rangle + |\bar\ell\ell\bar\ell\ell\rangle + |\bar\ell\bar\ell\ell\ell\rangle \quad (4)$$

which is the symmetric Dicke state of $N = 4$ photons with $N/2 = 2$ excitations. This state is in particular interesting as it is robust to photon losses and has the largest distance from not genuine multipartite entangled states.[27] Entanglement in such states can easily be verified by measuring the total collective spin along the x, y directions;[27] if $\langle \mathcal{W}_4^{(2)} \rangle = \langle J_x^2 \rangle + \langle J_y^2 \rangle > 5$ (for $N = 4$; $J_i = \frac{1}{2} \sum_k \sigma_i^{(k)}$ where, e.g., $\sigma_y^{(2)} = \mathbb{1} \otimes \sigma_y \otimes \mathbb{1} \otimes \mathbb{1}$), the state is non-separable, i.e., entangled. We obtain experimentally $\langle \mathcal{W}_4^{(2)} \rangle = 5.17 \pm 0.09$, thus verifying entanglement in the 4-photon OAM state.

$\langle \mathcal{W}_4^{(2)} \rangle$ can also be used to detect genuine multipartite entanglement,[14,15,28] if it violates $\langle \mathcal{W}_4^{(2)} \rangle \leq 7/2 + \sqrt{3} \approx 5.23$.[27] The proposed theoretical state in Eq. 3, for which $\langle \mathcal{W}_4^{(2)} \rangle = 6$, is indeed genuine multipartite entangled, but our experimental result does not violate this bound. We argue that experimental imperfections are responsible: Apart from spectral-filtering issues, we have here the extreme requirement that all 4 detectors have to be mode matched simultaneously. In contrast to experiments on polarization entanglement, here, even small misalignment does not only reduce count rates but also alters the measurement projectors by inducing small rotations in the respective single-particle Hilbert space, and the 4-fold mode-matching exponentially amplifies any misalignment. The experimentally obtained numerical values should therefore be seen as a lower limit only. We can correct for this partially if we have access to the full density matrix, as we show now.

We use tomographic quantum state reconstruction[29] to obtain the most likely density matrix ρ describing the detected state. Experimental integration time is 120 s for each detector setting, and we additionally combine the data with the more accurate measurements of the basis-state correlations shown in Fig. 3. In Fig. 4 we compare the resulting experimental density matrix to the theoretical expectation (Eq. 4). As a multipartite entanglement witness we use the one proposed in Ref. 30, which is also
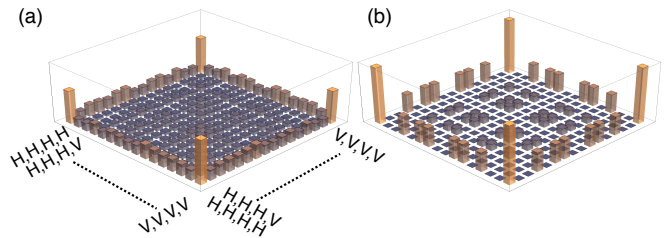

Figure 4. **The reconstructed OAM quantum state.** Modulus of the reconstructed experimental (a) and theoretical (b) density matrix (vertical axis scale: $[0 \dots 0.3]$). The discrepancy between experiment and theory is mainly caused by residual misalignment of the transverse-mode detectors.

more resilient against noise compared to the collective-spin witness above. Violation of the inequality $I_2^4[\rho] \leq 0$ indicates genuine multipartite entanglement of ρ. This witness is constructed such that it is optimal for the Dicke state with two excitations $|D_4^{(2)}\rangle$ and gives 1 in this case. For analysis of the experimental density matrix, we apply local single-qubit rotations and search for maximum violation of the witness (see methods). For 3 independently measured data sets, we obtain $I_2^4[\rho] = \{0.28, 0.32, 0.34\}$, thus giving strong indication of genuine 4-photon OAM entanglement.

We have studied here the zero- and first-order modes with $\ell = \{0, \pm 1\}$. Exploration of the rich correlations in the full higher-dimensional multipartite state (Eq. 2) will require higher pump beam intensities and therefore the use of nonlinear crystals with higher damage threshold, both within reach today. The 4-photon OAM entangled state that we have produced and characterized here might open new possibilities and protocols in multi-party quantum secret sharing[17] with Dicke states in the sense that here, more information per photon quadruplet can be exchanged or the security increased by the high-dimensional nature of the OAM or transverse-mode degrees of freedom.[18] Further, the spatial correlations carried by our multi-photon states might enable new options in quantum metrology, microscopy, and imaging.

Appendix

Photon quadruplet creation in high-gain SPDC:

We use a PPKTP crystal cut for degenerate collinear type-I SPDC. The photon pairs at 826 nm experience a different group index than the pump beam of 413 nm in PPKTP, therefore temporal labelling can occur. The group index difference is $n_g(2\omega) - n_g(\omega) = 0.456$ at 300 K, corresponding to a group velocity dispersion of $D = 1.5$ ps/mm, and a group velocity walk-off length $L_{gv} = 1.3$ mm for $\Delta t = 2$ ps pulses. Thus, we choose a 1 mm long crystal. We separate the pump beam with an anti reflection coated GaP plate and select a narrow frequency window around the degenerate wavelength of 826 nm with a 1 nm wide spectral filter.

The number of available entangled transverse modes is determined by the pump beam size in the crystal, at perfect phase matching. To achieve sufficient count rates, we focus the pump beam to $50\,\mu$m (while the detection mode waist in the crystal is $100\,\mu$m), which results in ~ 9 transverse modes.

If not noted otherwise, we use a pump power of 70 mW, which corresponds to a peak intensity at the focus of 11.2 kW cm^{-2}. This is close to the PPKTP damage threshold; above this, gray-tracking was observed. Elevated temperatures or other materials, such as periodically poled Lithium Niobate, would enable the use of higher intensities.

Entanglement witness optimization:

Local unitary transformations, complex basis rotations, are allowed to be applied to each part of a multipartite state without changing its entanglement properties. Most entanglement witnesses, including the witness for n particles $I_m^n[\rho]$ optimized for a Dicke state with m excitations from Ref.,[30] only detect entanglement optimally in a particular basis, and optimization over basis rotations has to be done. Here, we optimize $I_m^n[\rho]$ by transformation of the experimentally determined (or theoretical) density matrix ρ as follows: $\rho \to U\rho U^{\dagger}$, where $U = U_1 \otimes U_2 \otimes U_3 \otimes U_4$ with the generic unitary

$$U_i = \begin{bmatrix} \exp i\alpha_i \cos\gamma_i & \exp i\beta_i \sin\gamma_i \\ -\exp i(\alpha_i - \delta_i)\sin\gamma_i & \exp i(\beta_i - \delta_i)\cos\gamma_i \end{bmatrix}$$

for the real parameters $\{\alpha_i,\ \beta_i,\ \delta_i,\ \gamma_i\}$. These 16 parameters are simultaneously optimized using robust unconstrained numerical optimization routines.

* loeffler@physics.leidenuniv.nl

[1] Monz, T. *et al.* 14-Qubit Entanglement: Creation and Coherence. *Phys. Rev. Lett.* **106**, 130506 (2011).

[2] Yao, X.-C. *et al.* Observation of eight-photon entanglement. *Nat. Photon.* **6**, 225 (2012).

[3] Pan, J.-W. *et al.* Multiphoton entanglement and interferometry. *Rev. Mod. Phys.* **84**, 777 (2012).

[4] Shalm, L. K. *et al.* Three-photon energy-time entanglement. *Nat. Phys.* **9**, 19 (2013).

[5] Walborn, S. P., Lemelle, D. S., Almeida, M. P. & Ribeiro, P. H. S. Quantum Key Distribution with Higher-Order Alphabets Using Spatially Encoded Qudits. *Phys. Rev. Lett.* **96**, 090501 (2006).

[6] Lanyon, B. P. *et al.* Simplifying quantum logic using higher-dimensional Hilbert spaces. *Nature Phys.* **5**, 134 (2009).

[7] Hiesmayr, B. C. & Löffler, W. Complementarity reveals bound entanglement of two twisted photons. *New J. Phys.* **15**, 083036 (2013).

[8] Wieczorek, W. *et al.* Experimental Observation of an Entire Family of Four-Photon Entangled States. *Phys. Rev. Lett.* **101**, 010503 (2008).

[9] Mair, A., Vaziri, A., Weihs, G. & Zeilinger, A. Entanglement of the orbital angular momentum states of photons. *Nature* **412**, 313 (2001).

[10] Dada, A. C., Leach, J., Buller, G. S., Padgett, M. J. & Andersson, E. Experimental high-dimensional two-photon entanglement and violations of generalized Bell inequalities. *Nature Phys.* **7**, 677 (2011).

[11] Krenn, M. *et al.* Generation and confirmation of a (100 $\times$ 100)-dimensional entangled quantum system. *Proc. Natl. Acad. Sci. U.S.A.* **111**, 6243 (2014).

[12] Salakhutdinov, V. D., Eliel, E. R. & Löffler, W. Full-Field Quantum Correlations of Spatially Entangled Photons. *Phys. Rev. Lett.* **108**, 173604 (2012).

[13] Lamas-Linares, A., Howell, J. C. & Bouwmeester, D. Stimulated emission of polarization-entangled photons. *Nature* **412**, 887 (2001).

[14] Gühne, O. & Seevinck, M. Separability criteria for genuine multiparticle entanglement. *New J. Phys.* **12**, 053002 (2010).

[15] Huber, M., Mintert, F., Gabriel, A. & Hiesmayr, B. C. Detection of High-Dimensional Genuine Multipartite Entanglement of Mixed States. *Phys. Rev. Lett.* **104**, 210501 (2010).

[16] Popescu, S. Nonlocality beyond quantum mechanics. *Nature Phys.* **10**, 264 (2014).

[17] Hillery, M., Bužek, V. & Berthiaume, A. Quantum secret sharing. *Phys. Rev. A* **59**, 1829–1834 (1999).

[18] Yu, I.-C., Lin, F.-L. & Huang, C.-Y. Quantum secret sharing with multilevel mutually (un)biased bases. *Phys. Rev. A* **78**, 012344 (2008).

[19] Howell, J. C., Bennink, R. S., Bentley, S. J. & Boyd, R. W. Realization of the Einstein-Podolsky-Rosen Paradox Using Momentum- and Position-Entangled Photons from Spontaneous Parametric Down Conversion. *Phys. Rev. Lett.* **92**, 210403 (2004).

[20] Allen, L., Beijersbergen, M. W., Spreeuw, R. J. C. & Woerdman, J. P. Orbital angular momentum of light and the transformation of Laguerre-Gaussian laser modes. *Phys. Rev. A* **45**, 8185 (1992).

[21] Yorulmaz, S. C., van Exter, M. P. & de Dood, M. J. A. The role of spatial and temporal modes in pulsed parametric down-conversion. *Opt. Express* **22**, 5913 (2014).

[22] Padgett, M. J. & Courtial, J. Poincaré-sphere equivalent for light beams containing orbital angular momentum. *Opt. Lett.* **24**, 430 (1999).

[23] Ou, Z. Y. Distinguishing four photons in an entangled state from two independent pairs of photons. *Phys. Rev. A* **72**, 053814 (2005).

[24] van der Torren, A. J. H., Yorulmaz, S. C., Renema, J. J., van Exter, M. P. & de Dood, M. J. A. Spatially entangled four-photon states from a periodically poled potassium-titanyl-phosphate crystal. *Phys. Rev. A* **85**, 043837 (2012).

[25] Riedmatten, H. D. *et al.* Two independent photon pairs versus four-photon entangled states in parametric down conversion. *J. Mod. Opt.* **51**, 1637 (2004).

[26] Simon, C., Weihs, G. & Zeilinger, A. Optimal Quantum Cloning via Stimulated Emission. *Phys. Rev. Lett.* **84**, 2993 (2000).

[27] Tóth, G. Detection of multipartite entanglement in the vicinity of symmetric Dicke states. *J. Opt. Soc. Am. B* (2007).

[28] Bourennane, M. *et al.* Experimental Detection of Multi-partite Entanglement using Witness Operators. *Phys. Rev. Lett.* **92**, 087902 (2004).

[29] James, D. F. V., Kwiat, P. G., Munro, W. J. & White, A. G. Measurement of qubits. *Phys. Rev. A* **64**, 052312 (2001).

[30] Huber, M., Erker, P., Schimpf, H., Gabriel, A. & Hiesmayr, B. Experimentally feasible set of criteria detecting genuine multipartite entanglement in n -qubit Dicke states and in higher-dimensional systems. *Phys. Rev. A* **83** (2011).